International Conference on Space Optics—ICSO 2010

Rhodes Island, Greece

4–8 October 2010

Edited by Errico Armandillo, Bruno Cugny, and Nikos Karafolas

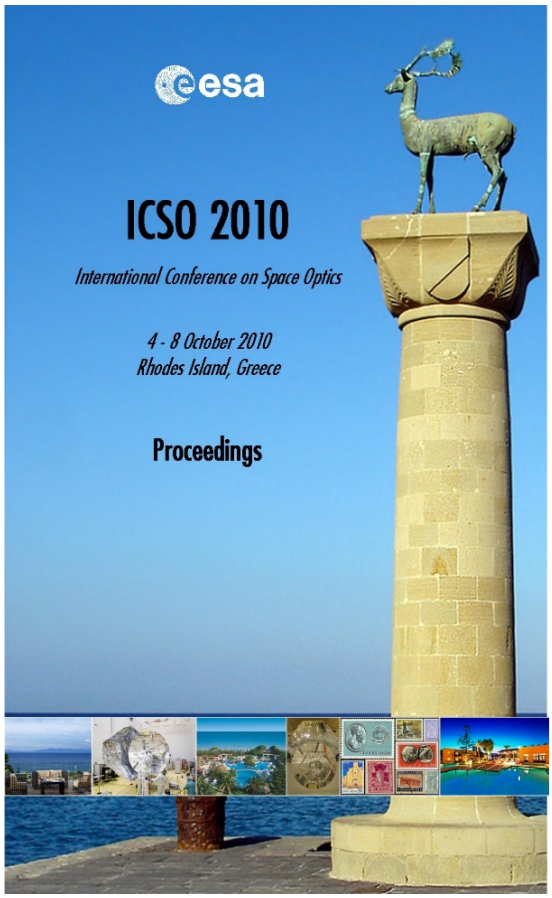

Interferometric system for pm-level stability characterization

A. L. Verlaan, J. D. Ellis, D. Voigt, J. W. Spronck, et al.

International Conference on Space Optics — ICSO 2010, edited by Errico Armandillo, Bruno Cugny, Nikos Karafolas, Proc. of SPIE Vol. 10565, 1056569 · © 2010 ESA and CNES
CCC code: 0277-786X/17/$18 · doi: 10.1117/12.2552558

INTERFEROMETRIC SYSTEM FOR PM-LEVEL STABILITY CHARACTERIZATION

A. L. Verlaan[1], J. D. Ellis[2], D. Voigt[3], J. W. Spronck[2], R. H. Munnig Schmidt[2]
[1]*TNO Science & Industry, Delft, The Netherlands*
[2]*PME: Mechatronic System Design, Delft University of Technology, Delft, The Netherlands*
[3]*VSL Dutch Metrology Institute, Delft, The Netherlands*

ABSTRACT

We present a double sided, single pass Michelson heterodyne interferometer for dimensional stability measurements. In preliminary measurements, the double deadpath configuration (no sample) showed better than ±1.5 nm (2σ) over 13 hours. A 30 mm stainless gauge block was then measured with a stability of ±1.2 nm (2σ) over 9 hours. The interferometer was then moved to a facility capable of measuring in vacuum. In a pressure sealed environment, but not vacuum, the interferometer stability was better than ±0.6 nm (2σ) over 23 hours. Using a Fourier analysis on this drift measurement, the limiting factor is the slight spatial gradients in the refractive index. With relatively large air paths greater than 400 mm, refractive index fluctuations on the order of parts in 10^9 are needed to cause this drift.

I. INTRODUCTION

Material, interface, and construction stability are important parameters for space instrumentation, (EUV-) lithography, and metrology in general. In both EUV lithography and space, more information is needed about material and mechanical connection stability during an atmospheric to vacuum transition, after thermal and mechanical cycling, and over time (drift). With space missions like LISA and GAIA, the stability requirements on both materials and constructions become more and more stringent and the time scales over which these stabilities are required increase as well. Presently, there is a lack of knowledge of material and construction stability to build these instruments to their requirements. As a first step, a measurement system with high resolution and low measurement uncertainty is required for the investigation into material stability. We are investigating an instrument for measuring length changes of a 50 mm long sample with a 10 pm (k=2) measurement uncertainty for 10 minute measurements and 100 pm (k=2) uncertainty for 1 day measurements.

II. INTERFEROMETER CONCEPT

We have developed a single-pass, double-sided interferometer, shown in Fig. 1, for measuring material stability [1]. A double-sided design was chosen because it eliminates the length change uncertainty due to the reference plate mounting [2]. With this design, the reference signal in the interferometer can also be used as a refractometer, which allows for the localized measurement of refractive index changes. This is a significant improvement (low uncertainty) over calculating the refractive index from environmental parameters [3]. This interferometer uses two spatially separated beams with a known frequency difference between the beams. These two beams are split equally forming eventually two different interference signals: one that measures the sample length change and the other that is a refractometer. The only optical path difference between the sample interferometer and refractometer interferometer is the slight spatial separation and the difference between the sample length and the vacuum tube length.

Two spatially separated beams with the same polarization state and a slight frequency offset are used as the source for this interferometer. The reference beam (blue in Fig. 1) enters the interferometer in the top plane (see Front View, Fig. 1). It is split using a 45° turned beamsplitter with a special coating ensuring equal power output for the transmitted and reflected beams. The two ensuing beams are the *refractometer-reference* (RR) and the *sample-reference* (SR), with equal power. Both the RR and SR beams pass through PBS_1, Q_1, and Q_2. After passing through Q_1 and Q_2, the polarization state is rotated 90°, where the beams reflect off PBS_2. The beams then reflect off M_2, M_1, and PBS_1, where they pass through Q_1 and Q_2 for a second time. The polarization state is rotated back to the original 0° and the beams transmit through PBS_2. Here, the beams are split equally in a LDBS, where they are interfered with their respective measurement arm.

The measurement beam (red in Fig. 1) enters the interferometer in the bottom plane and pass through the same rotated BS generating the *sample-measurement* (SM) and the *refractometer-measurement* (RM) beams. The RM beam follows the same nominal path as the RR and SR beams. It makes two passes in the interferometer, each time passing through a vacuum tube before exiting PBS_2. When it enters the LDBS it is reflected upward and

then interfered with the RR beam at the 50% beamsplitter surface. PD_r is then used to measure the fluctuations in the interferometer, as well as changes in the refractive index.

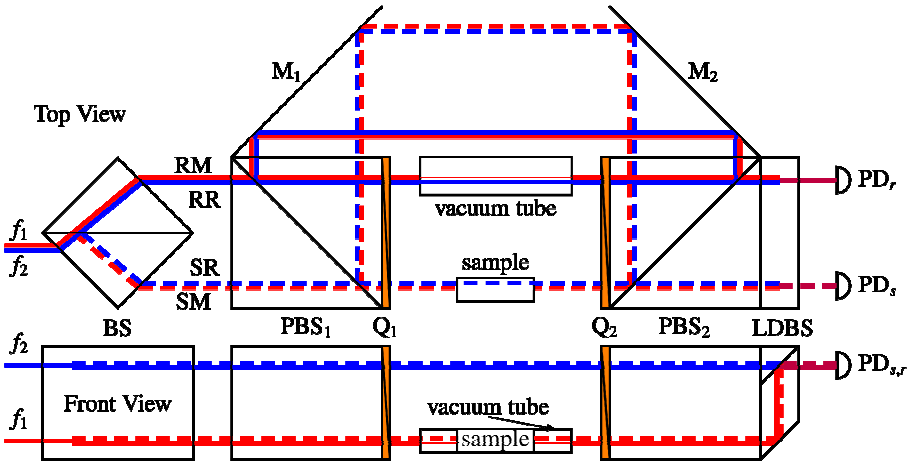

Fig. 1. Schematic of the double sided, signal pass interferometer used in the research. The solid beams interfere with each other to generate a refractometer. The dashed beams interfere to measure sample length changes. The input beams are spatially separated with the same polarization state with an offset frequency to eliminate periodic nonlinearity. (BS, beamsplitter; $PBS_{1,2}$, polarizing beamsplitter; $Q_{1,2}$, quarter wave plate; $M_{1,2}$, mirrors; VT, vacuum tube; LDBS, lateral displacement beamsplitter; $PD_{r,s}$, photodetectors)

The SM beam follows a slightly different path than the other three beams. The SM beam passes through PBS_1 and Q_1, where it then reflects off the left side of the sample. The beam then passes back through Q_1, where the polarization state is rotated 90°. The SM beam then reflects off PBS_1, M_1, M_2, and PBS_2. After this, the beam passes through Q_2 and reflects off the right side of the sample. The beam then passes back through Q_2 and now transmits through PBS_2. The beam is then reflected upwards in the LDBS where it is interfered with the SR beam at the 50% beamsplitter surface. PD_s is then used to measure sample length changes, as well as interferometer and reflective index changes.

A third detector, not shown, is used to generate an optical (heterodyne) reference. The phase difference between the optical reference and the refractometer is measured and used to determine refractive index fluctuations. The phase difference between the optical reference and the sample measurement signal is used to determine sample length changes. After correcting for sample thermal expansion and pressure induced length changes, the difference between the refractometer measurement and the sample measurement is used to determine the drift which includes corrections for refractive index changes and interferometer instability.

The source for this system contains a stabilized laser and two acousto-optic modulators (AOM) to generate spatially separated beams without frequency mixing, as shown in Fig. 2. The stabilized laser is a custom 3-mode stabilized laser with a fraction frequency stability better then 1 part in 10^{10} [4,5]. This stabilized laser has greater than 2 mW of useable power for the interferometer. The beam from this laser is then split equally and sent to two AOMs which are driven by 19.99 MHz and 20 MHz signals, creating a 10 kHz heterodyne beat frequency.

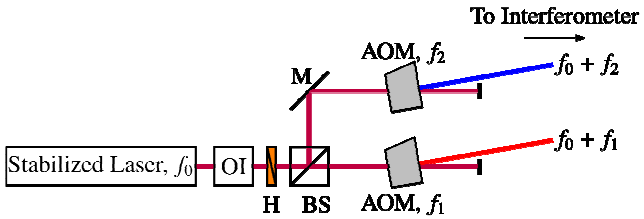

Fig. 2. Laser source and heterodyne frequency generating system used in the vacuum vessel experiments. A custom 3-mode stabilized laser with 2 mW of power and fractional frequency stability better than 1 part in 10^{10} was used as the source [4]. The polarization state is then aligned using H and then the laser is split equally. Two AOMs at slightly difference frequencies are then used to generate the f_1 and f_2 beams. (OI, optical isolator; BS, beamsplitter; H, half wave plate; AOM, acousto-optic modulator; M, mirror)

III. PRELIMINARY EXPERIMENTS

Preliminary experiments were performed in a double deadpath configuration. In this configuration, neither a sample nor a vacuum tube was used in the interferometer. This means the reference arms see essentially the same path as the measurement arms, with the exception in the LDBS. This, however, is corrected by using an appropriate LDBS in the opposite configuration in the source which splits the system into measurement and reference beams. This double deadpath configuration is the most basic setup for this interferometer and is used to establish a baseline noise level and to see whether common perturbations can be canceled and/or corrected.

The results, shown in Fig. 3, show the two deadpath interferometers drift approximately 500 nm over 13 hours with 0.3 K and 300 Pa temperature and pressure fluctuations, respectively, over the same timeframe. The measured length change between the two deadpath interferometers was strongly correlated. The difference between the two interferometers was within ±1.5 nm (2σ). The noise in the measurement was likely due to residual temporally fluctuating spatial refractive index gradients in the beam paths. The each of the four beam paths (SM, SR, RR, RM) were about 400 mm in length each which corresponds to refractive index coupling between each beam to better than 2.5 parts in 10^9.

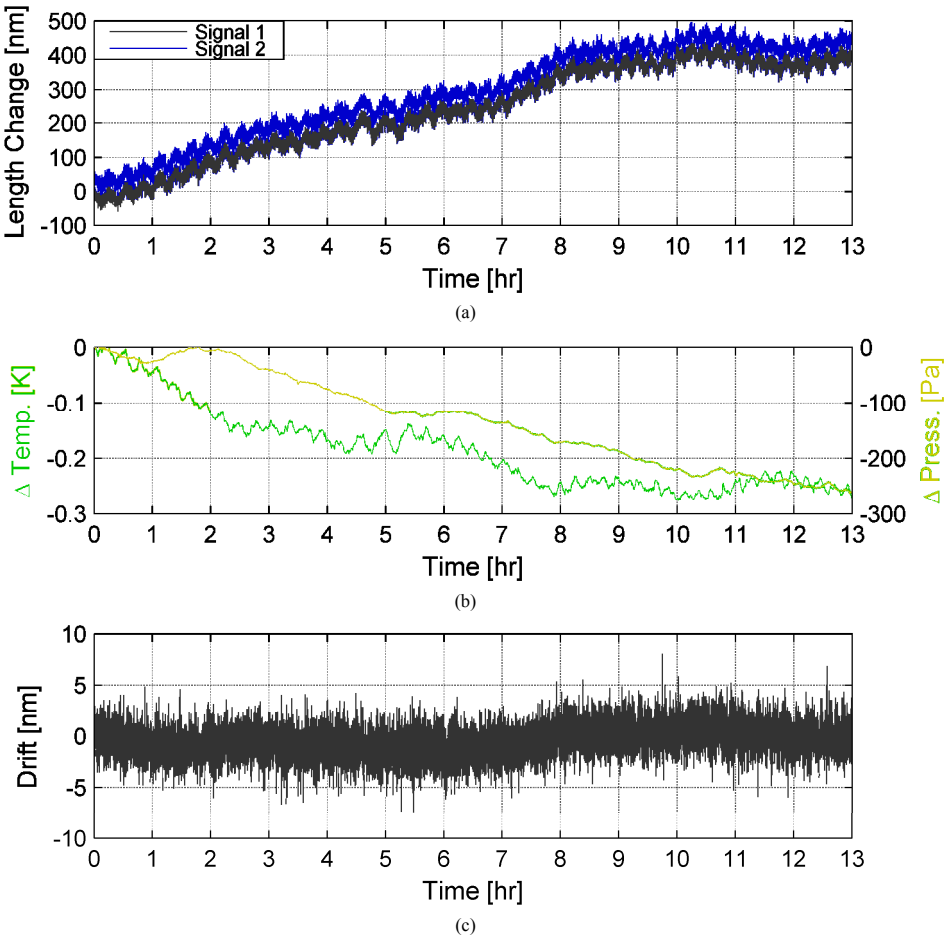

Fig. 3. (a) Length change of the two deadpath signals in the interferometer. The two signals are offset in the Y-axis for clarity. (b) Temperature and pressure fluctuations during the measurement. The interferometer was placed in an insulation foam box to limit air currents and temperature fluctuations. (c) Measured drift (difference between the two deadpath interferometers) of the double deadpath interferometer. The noise is about ±1.5 nm (2σ).

After measuring the deadpath, a 30 mm stainless steel gauge block (as an example) was measured over 9.5 hours. The reference signal was still the deadpath (no vacuum tube was used). The results, shown in Fig. 4, show a significant difference between the measurement signal and the reference signal. There also is a high frequency component contributing large noise level of approximately 50 nm pk-pk. However, this noise level is common to both signals and is significantly reduced when the difference is taken.

The air temperature and gauge block temperature were measured to correct for refractive index changes and to compensate for thermal expansion effects. In Fig. 4c, the one measurement and four different correction parameters are shown. First, the measured phase difference (φ) is the difference between the measurement and reference signals. This should be compensated for four different effects to reduce the measured drift value. These are from the laser frequency stability (freq), refractive index (RI) calculated using the temperature and pressure sensitivity coefficients reported by Estler [6], sample thermal expansion changes (CTE), and pressure induced length changes (press).

After removing these effects for the measured phase change, the 30 mm gauge block drift was better than 6 nm pk-pk over 9.5 hours, as shown in Fig. 4d. This corresponds to a similar noise level and drift level seen in the preliminary deadpath experiments. Since the vacuum tube was not used in these experiments, the refractive index variations accounted for by temperature and pressure measurements.

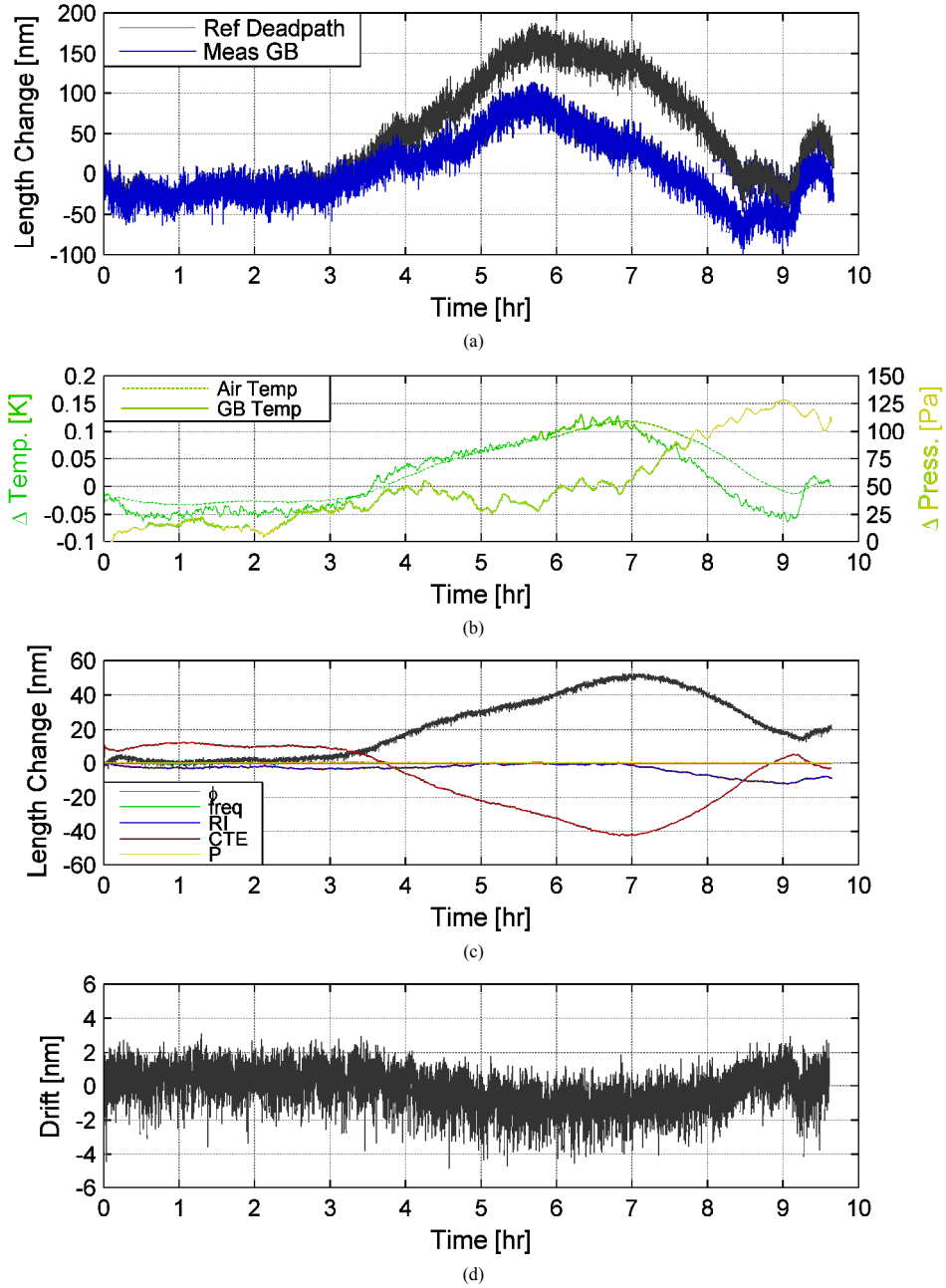

Fig. 4. (a) Measured length change of the two signals in the interferometer. The large difference is due to sample length change effects. (b) Temperature of the air and gauge block (GB) and pressure changes during the measurement. (c) Phase change between the measurement and reference signals and four correction curves from sample properties, environmental parameters, and laser stability. (d) Drift of a 30 mm stainless steel GB after correcting for temperature, pressure, refractive index, and laser stability effects.

These experiments were performed with a slightly different interferometer source. A beam from the 3-mode laser was split equally and one portion was frequency upshifted 20 MHz. This beam and original beam from the laser were used as the input to the interferometer. After detecting 20 MHz interference signals, each signal was mixed with a common oscillator at 19.99 MHz and filtered to generate 10 kHz signals where the phase was detected using a dual lock-in amplifier.

IV. VACUUM VESSEL EXPERIMENTS

The interferometer setup was moved to a different facility to implement measurements in a vacuum vessel. Prior to measuring in vacuum, the double deadpath setup was measured again to verify previous results. Fig. 5 shows the measurement results from the double deadpath setup in the vacuum vessel.

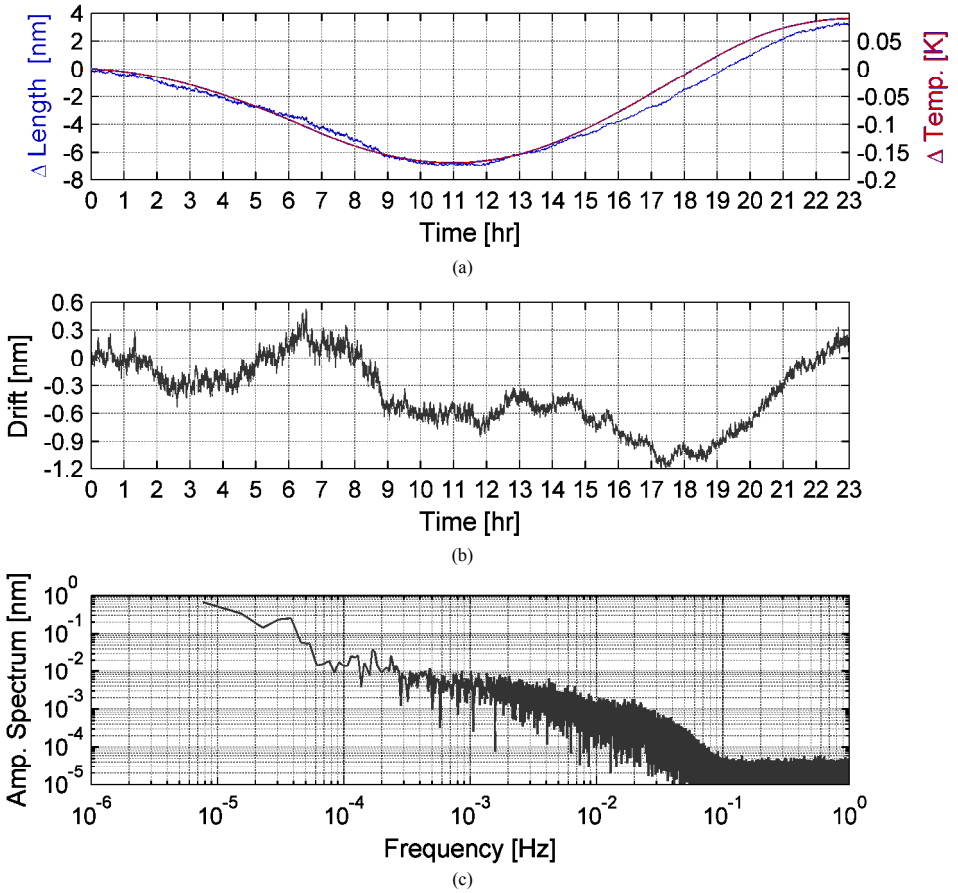

Fig. 5. (a) Comparison between the length change difference between the two deadpath interferometers and the measured temperature in the vacuum vessel over 23 hours. (b) Measured drift of the double deadpath interferometer over 23 hours after correcting for thermal fluctuations. (c) Single sided amplitude spectrum showing minimal disturbances above 0.1 Hz. The 1/*f* noise below 0.1 Hz is limited by refractive index perturbations in the beam paths.

The length change difference between the two interferometer deadpath interferometers was strongly correlated to the temperature within the vacuum vessel. After removing the correlation, the measured drift was better than ±0.6 nm (2σ) over 23 hours. The limit of this measurement is slight refractive index variations between the different beams within the interferometer. This is known to occur at frequencies below 0.1 Hz, shown in Fig. 5c, which was apparent as well in other measurements with this system.

The correlation between the deadpath interferometer difference and the temperature change is likely due to subtle changes to the interferometer when reconfiguring the setup to be hosted in the vacuum vessel. The stabilized laser was fiber fed into the vessel. Both AOMs were placed in the vessel and near the interferometer due to space limitations. Also, three detectors were used in the vessel, which also contribute as heat sources. Lastly, some of the mounted components were switched, which is also likely source for differences between these results and previous results.

The heat sources in the vacuum vessel will create slight air currents in the interferometer even though the system was pressure sealed. These air currents, combined with a relatively large optical path length (> 400 mm) per arm (x4 arms) means only slight refractive index variations are needed to cause these errors. Refractive index variations on the order of 10^{-10} are needed to create these errors.

V. CURRENT STATUS

Currently, the interferometer is undergoing experiments in a low vacuum environment to limit air currents and refractive index changes. At present, the interferometer is has been in a 3 mbar environment for 13 hours with less than 6 nm of total drift. As the system still needs time to stabilize, we expect this drift will taper off to sub-nanometer levels. The noise level on top of the drift has also decreased from 25 pm in the previous double deadpath measurement in the vacuum vessel to better than 12 pm.

VI. CONCLUSIONS

This interferometer is currently capable of measuring nanometer level drift over a day. Using the second interferometer (refractometer) as a deadpath interferometer reference eliminates much of the high frequency noise due to optical mounts and vibrations. The limit factor for this system was the refractive index which contributed to errors at frequencies below 0.1 Hz due to residual temporally fluctuating spatial refractive index gradients in the beam paths. Even so, with 400 mm long beam paths, a 30 mm spatial separation between interferometers, and 20 mm spatial separation between reference and measurement arms per interferometer, the refractive index coupling between beams is better than a few parts in 10^9.

The authors would like to thank the Dutch IOP for funding this research, project IP06104.

REFERENCES

[1] J.D. Ellis, K.-N. Joo, J.W. Spronck, and R.H. Munnig Schmidt, “Double-sided interferometer with low drift for stability testing,” *In: Proceedings of the 9th International Symposium on Measurement technology and intelligent Instruments,* 29 June – 2 July, St. Petersburg, Russia, 2009.
[2] R. Schödel. “Ultra-high accuracy thermal expansion measurements with PTB's precision interferometer,” *Measurement Science and Technology*, vol. 19, no. 084003, 11pp, 2008.
[3] K.P. Birch and M. J. Downs, “An updated Edlén equation for the refractive index of air,” *Metrologia,* vol. 30, pp. 155-162, 1993.
[4] J.D. Ellis, K.-N. Joo, E.S. Buice, and J.W. Spronck, “Frequency stabilized three mode HeNe laser using nonlinear optical phenomena,” *Optics Express*, vol. 18, no. 2, pp. 1373–1379, 2010.
[5] J.D. Ellis, K.-N. Joo, E.S. Buice, J.W. Spronck, and R.H. Munnig Schmidt, “Frequency stabilization and heterodyne system via the mixed mode in three mode HeNe lasers,” *In: Proceedings of the 10th euspen International Conference,* 31 May - 3 June, Delft, The Netherlands, 2010
[6] W.T. Estler, “High-accuracy displacement interferometry in air,” *Applied Optics,* vol. 24, pp. 808-815, 1985.